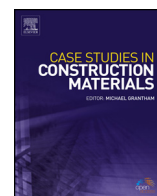




ELSEVIER

Contents lists available at ScienceDirect

Case Studies in Construction Materials

journal homepage: www.elsevier.com/locate/cscm

Short communication

Durability study of concrete incorporating dredged sediments

Raouf Achour^{a,b,*}, Rachid Zentar^a, Nor-Edine Abriak^a, Patrice Rivard^b,
Pascal Gregoire^c^a Ecole Mines Télécom de Douai, GCE, 764 Bd Lahure, BP 10838, 59508 Douai, France^b Department of Civil Engineering, Université de Sherbrooke, Canada^c Grand Port Maritime de Dunkerque, France

ARTICLE INFO

Article history:

Received 26 November 2018

Received in revised form 19 April 2019

Accepted 6 May 2019

Keywords:

Characterisation

Concrete accropode blocks

Dredged sediments

Durability

External sulphate attack

Freeze/thaw

ABSTRACT

Every year, significant volumes of marine sediment are dredged from the harbour of Dunkirk, France. These materials may in fact be used beneficially in the composition of new concrete accropode blocks to protect the harbour coastline.

This paper evaluates the mechanical behaviour and durability of accropode blocks composed of concrete and dredged fine sediments after three years of storage on a dock at port of Dunkirk. A description of accropode blocks, a coring campaign and characterisation of cylindrical core samples are presented and discussed. To assess the durability of the concrete, a battery of accelerated tests is performed. The mechanical properties of various core samples are measured during durability tests using non-destructive techniques.

The results suggest that sediment addition should be limited to 12.5% of the concrete mix to ensure the integrity of mechanical properties under external sulphate attack and frost action.

© 2019 Published by Elsevier Ltd. This is an open access article under the CC BY-NC-ND license (<http://creativecommons.org/licenses/by-nc-nd/4.0/>).

1. Introduction

The main objective of this study is to explore alternative solutions to managing dredged fine sediment sand as a new source of supply in the field of maritime works. This need is increasing with the impacts of climate change in terms of rising sea level and its impact on the coastal shoreline.

In the last two decades, several studies have been carried out to validate the use of sediments in various applications: road construction [1–8], brick manufacture [9,10], mortar production [11], concrete production [12,13], and cement production [14,15]. However, these applications require use of the material in an environment different from its origin. Such usage can induce harmful impacts on the environment, such as pollution from transport if the site of use is far from the coastal shoreline, or contamination of the site of use from the release of salts contained in the sediments.

In this study, the proposed field for valorisation is the manufacture of concrete accropode blocks to be used in protecting maritime infrastructure. Use of traditional aggregates to develop protection systems can induce harmful impacts on the environment due to over exploitation of quarries, shortage of aggregates, and transportation of materials to the area of use. Use of dredged sediments as a substitute for traditional aggregates could provide a number of advantages: improved management of dredged sediments, efficiency/ease of access to resources at site of use, and prevention of harm caused by the resource as it is used in its original environment. Given these possibilities, Dunkirk has launched several studies, with the help of research laboratories and industrial partners, to explore the use of dredged sediments as a substitute for traditional

* Corresponding author.

E-mail address: achour.raouf1@gmail.com (R. Achour).

aggregates in concrete or as a substitute in cement [8,11,16,17]. However, the durability of the developed material has been studied only very briefly [17–19].

In the present study, the durability of concrete is tested on two accropode blocks with different amounts of fine sediments incorporated into their design. Prior to this study, the two blocks were stored for three years on a dock at port of Dunkirk.

This durability study was created to assess the effect of external sulphate attack and freeze/thaw cycles on the mechanical properties of the material. For both types of tests, different procedures were compared.

2. Materials, methodology and experimental program

The concrete blocks from which cylindrical specimens were prepared were made in 2010. These blocks were designed to protect and reinforce the breakwater dykes in Dunkirk harbour. The blocks have undergone various cycles of immersion and emersion. In 2012, a core drilling campaign was conducted on the two blocks according to the European standard NF EN 12 504 -1 [20]. The block types differ in the amount of dredged sediments included in the concrete mix. Sample C1 contains 12.5% dredged fine sediments, and sample C2 contains 20% dredged fine sediments. It is of note that during the initial design of the present study, substitution of less than 12.5% was declared non-economical from the point of view of sediment management, while substitution of 20% was shown to be the maximum limit for maintenance of adequate mechanical and rheological properties during pouring and in terms of targeted strength.

The experimental program undertaken is summarized in Fig. 1. The test program includes an initial characterisation study of samples after coring (destructive tests and non-destructive tests), characterisation of the samples during durability tests (non-destructive tests) and finally a series of tests at the end of the durability tests (destructive tests and non-destructive tests).

2.1. Composition of accropodes

Table 1 provides the composition of the concrete accropodes investigated in this paper. The marine sediments were dredged from the port of Dunkirk (Grand Port Maritime de Dunkerque, France). The same marine sediment was previously used for a road valorisation study [5].

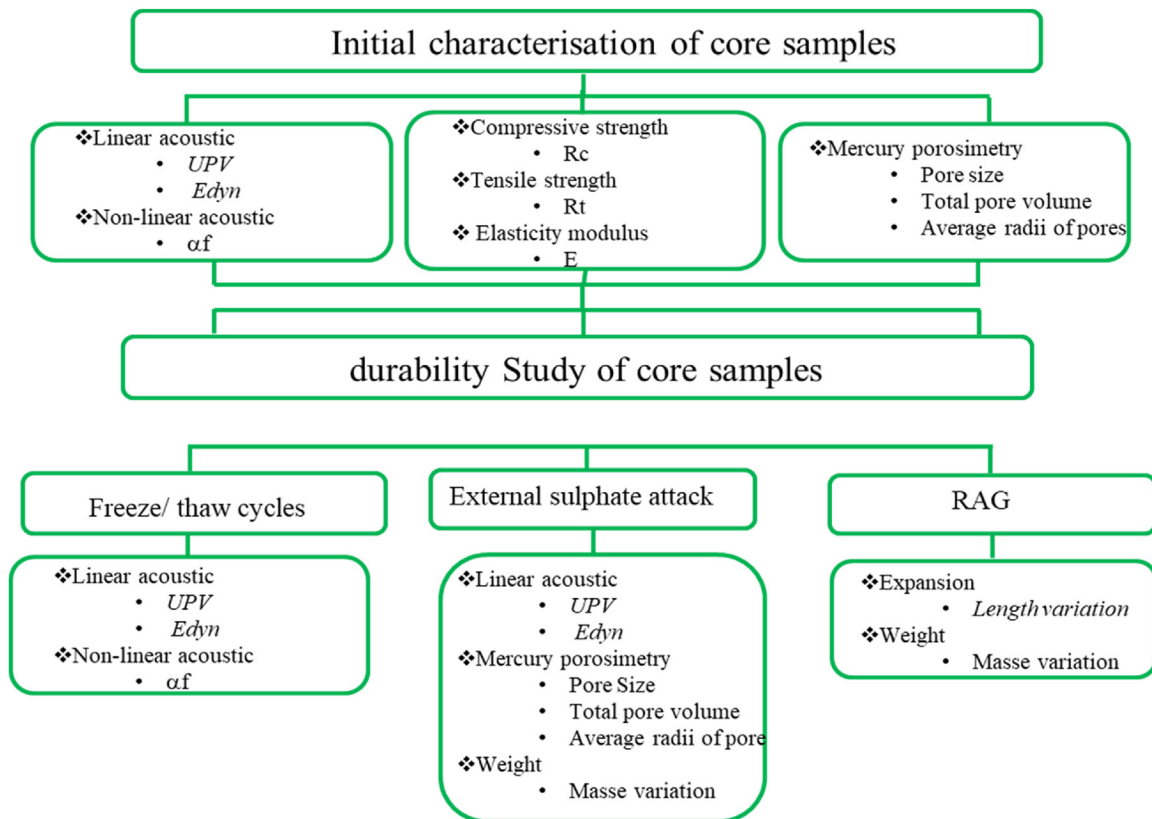


Fig. 1. Experimental program for the characterisation of samples C1 and C2. (UPV: ultrasonic pulse velocity; Edyn: dynamic modulus of elasticity; DRX: X-ray diffraction; αf: frequency shift.)

Table 1
Composition of the accropodes concrete C1 & C2.

Composition of concrete (Kg/m ³)	Concrete C1 (containing 12.5% marine sediment)	Concrete C2 (containing 20% marine sediment)
CEM I 52. PM	362	355
Marine sediment	221	381
0–4 mm Siliceous Sand	599	412
4–20 mm Aggregate	824	792
Water	221	295
Admixture	4.7	7

According to the initial study design, concrete incorporating 12.5% marine sediment was considered non-economical from the point of view of sediment management, while concrete incorporating 20% marine sediment was considered to be the maximum limit for acceptable mechanical and rheological properties.

2.2. Mechanical tests

In the initial characterisation of the core samples, destructive test types consisted of longitudinal and splitting tensile strength tests on the cylindrical samples. During these tests, the Young modulus of the sample was also measured. The compressive tensile strength and static modulus of elasticity were determined according to the standard tests ASTM C 39-02 [21], ASTM C 496-04 [22] and ASTM 469-02 [23], respectively. The reported results of these tests are the average values of three measurements. To determine the effects of the added marine sediment on the properties of the porous structure, an evaluation of the microstructure was carried out by measuring porosity with a Micromeritics AutoPore IV mercury porosimeter. It is of note that pore distribution is correlated not only to the strength of concrete but also has an important impact on its durability [24,25].

2.3. Non-destructive tests

To qualify the two types of concrete, in parallel to the destructive tests, non-destructive tests were carried out. Measurements were taken using two different techniques: linear acoustic testing (UPV: ultrasonic pulse velocity) and nonlinear acoustic testing (nonlinear resonance).

The primary goal of non-destructive tests (NDTs) is to provide an assessment of the quality of a material, whatever its age and condition. Linear acoustic techniques, such as linear resonance prescribed by ASTM C 215-02 [26], and ultrasonic pulse velocity (UPV) testing prescribed by ASTM C 597-97 [27] are among the most commonly used NDTs in civil engineering [28]. UPV provides a quick and easy way of estimating the elastic properties of a concrete, which can be associated with its strength. This technique measures the propagation time of compression (longitudinal) waves through the concrete sample (direct transmission).

Nonlinear resonance tests were performed with the experimental device shown in

Fig. 2. The full and detailed procedure can be found in Kodjo [29]. Fast dynamic nonlinear acoustics have proven their effectiveness for characterizing concrete and its degree of degradation. In contrast to linear acoustics, nonlinear acoustics use high amplitude waves capable of introducing locally substantial deformations in the medium as they propagate, thereby modifying the medium's mechanical properties and causing non-linear behaviour. These nonlinear acoustic tests provide parameters that are sensitive to micro-cracks. The device used to characterise the marine-sediment-based cores was developed at the University of Sherbrooke [29].

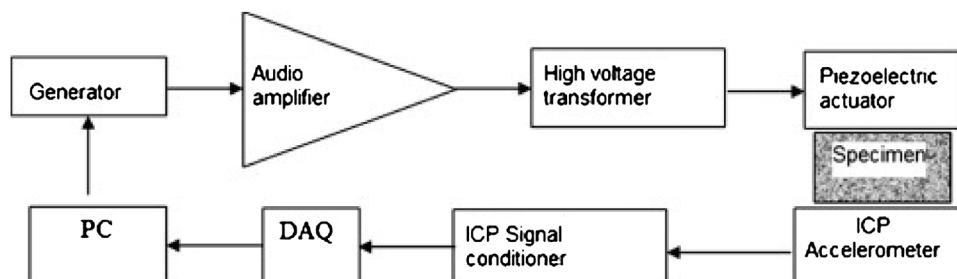


Fig. 2. Experimental device used for nonlinear acoustic testing.

2.4. Freeze/thaw tests

The durability of the cored samples was assessed by conducting a series of freeze/thaw cycles, external sulphate attacks and tests for alkali-aggregate reaction.

For freeze/thaw tests, samples of C1 and C2, each measuring 100 mm in diameter and 200 mm in length, were prepared and placed in a temperature-controlled chamber simulating for 24 h a freezing/thawing cycle between -18°C and 4°C in compliance with the ASTM C666 standard [30].

2.5. External sulphate attack

External sulphate attack on cement-based materials has been a key durability issue and the subject of extensive investigation for many decades [31]. There is a general consensus that dissolved sulphate salts can enter into chemical reactions with hydrated cement-based materials, causing expansion, cracking and spalling, and/or softening and disintegration. The classical form of sulphate attack involves alkali sulphates such as sodium sulphate (Na_2SO_4) which reacts with portlandite (CH), mono-sulphate and unreacted C_3A to form gypsum (CSH) and ettringite ($\text{C}_6\text{A S}_3\text{H}_{32}$), which can cause expansion, cracking, and deterioration of concrete. Yet, the exact mechanism of expansion and the role of gypsum and ettringite in the deterioration process remain subjects of controversy [32–34].

For the sulphate attack test, samples immersed in a 5% $\text{Na}_2\text{SO}_4 \cdot 10\text{H}_2\text{O}$ solution are subjected to wetting and drying cycles to accelerate the damage caused by salt crystallization in the pores of the concrete. The effects of this exposure can be measured by the loss of mass, strength and dynamic modulus of elasticity of the samples and by the expansion of the concrete [35]. Wetting and drying protocol is explored in three different ways. The first protocol consists of total immersion (without a drying stage). The second protocol combines wetting with drying at 60°C and the third protocol combines wetting with drying at 105°C . The $\text{Na}_2\text{SO}_4 \cdot 10\text{H}_2\text{O}$ solution is renewed every 30 days for all protocols.

Drying at 60°C accelerates the effect of total immersion, without making the test as severe as drying at 105°C . The temperature 105°C was selected to maximize the effect of immersion drying cycles and thus obtain the fastest ageing process. The only drawback is the risk of an internal sulphate attack, hence the alternate option of a lower temperature. The temperature 60°C was selected because the combination of both internal and external sulphate attacks is impossible. The delayed formation of the ettringite has never been found below 65°C [44].

2.6. Alkali-aggregate reaction

Alkali-aggregate reaction has been causing the expansion and cracking of numerous concrete structures worldwide. Alkali-aggregate reaction occurs between the alkali hydroxides (Na, K –OH) dissolved in the concrete pore solution of hydrated cement paste and certain reactive siliceous mineral phases of aggregates [36]. The expansion is due to the formation of continuing chemical reaction products, silica gels. These expansive gels create internal stresses and lead to the formation of a micro-crack network through the concrete when material tensile strength is reached. Moreover, gels have a viscous behaviour; under external and internal stresses, they slowly move into porous spaces and cracks and enhance the hysteretic behaviour of concrete.

For alkali-aggregate reaction (AAR), the methods currently used in North America are the Canadian CSA A23.2–14 A [37] or the American ASTM C1293 [38] concrete prism test. Since concrete specimens were kept at 38°C in high moisture conditions (>95% RH), length change and mass variation of samples C1 and C2 were measured periodically following the provisions of CSA A23.2–14 A.

3. Results and discussions

3.1. Characterisation of concrete prior to accelerated durability tests

Uniaxial compression tests were carried out in accordance with the ASTM C 39-02 standard. Sample cylinders C1 and C2 showed strengths of 40 MPa and 31 MPa, respectively (Table 2). Tensile strength was measured in accordance with the ASTM C 496-04 standard. The values were 3.6 and 3.3 MPa for samples C1 and C2, respectively. As already noted for compressive strength, with the addition of sediment a drop in tensile strength was observed. The modulus of elasticity was evaluated according to ASTM C 469-02 on samples of 100×200 mm. The results also showed a systematic drop between concrete C1

Table 2
Mechanical characterisation of tested core samples under destructive tests.

	C1	C2	% decrease
Compression strength ASTM C 39-02 (MPa)	40	31	22.5 %
Indirect tensile strength ASTM C 496 (MPa)	3.6	3.3	8.3%
E (GPa) ASTM C 469-02	30	26	13.3%

and C2. Hence, the increase from 12.5% to 20% dredged sediment in the concrete induced a decrease of all mechanical properties, which is likely an issue in terms of durability.

Two possibilities may explain this drop in mechanical properties. The first possibility is that the high porosity of marine sediments may increase the porosity of the concrete. The second possibility is that sediments may be weaker than natural aggregates.

For non-destructive characterisation of the two concretes, UPV (ultrasonic pulse velocity) was measured on 6 samples (3 samples per type of concrete) in accordance with the ASTM C 597-97. The results (see Table 2 below) show that the C1 sample reached a velocity of 3900 m/s, indicating a higher-quality concrete. The increase in amount of sediment by 7.5% in the C2 sample causes a drop of 300 m/s in UPV, indicating a lower-quality concrete. UPV demonstrated the sensitivity of this measurement to the different mechanical properties of the samples. This sensitivity can be used to assess differences in mechanical properties during durability tests.

The dynamic modulus of elasticity of samples C1 and C2 was calculated from their transverse and longitudinal resonant frequencies. As shown in Table 2 below, C1 (33 GPa) has a higher modulus than C2 (28 GPa). The decrease in the dynamic modulus of elasticity value is also associated with the increase of marine sediment (Table 3).

The parameter αf , which defines the frequency offset in the nonlinear resonance tests, was measured on both types of concrete. The results showed that C2 has a higher frequency offset αf than C1 (10,338 vs. 8272). Increasing the percentage of sediment from 12.5% to 20% leads to a significant increase in the nonlinear behaviour of the concrete. Previous studies reported that an increase in nonlinear behaviour is associated with a softening of the concrete and a loss of general mechanical properties [39,40].

To explain the impacts of sediment addition on microstructural changes induced in the concrete, Mercury Intrusion Porosimetry (MIP) tests were conducted. The MIP test allows measurement of pore-size distribution curves, quantitative pore volume, and average and median pore radii. Figs. 3 and 4 show the porosity measured for each type of concrete. The results clearly show an increase in total porosity with the increase of the amount of sediment. C1 has a total porosity of 11.6%, whereas C2 has a porosity of 16.9%. The effect of sediment addition is also marked with regards to the pore sizes.

Fig. 5 shows the distribution of the average pore diameter. The average pore diameter is about 42 nm for C1 and about 66 nm for C2. Ordinary concrete has an average pore diameter of 53 nm [41]. Total porosity shows that C1 is comparable to an ordinary concrete and has a finer pore network than ordinary concrete [40]. The addition of 12.5% marine sediments in the concrete mix provides microstructural characteristics comparable to ordinary concrete. The above results indicate that pore size increases with the amount of sediment. The addition of a higher proportion of marine sediment has modified the microstructure in C2, increasing the porosity and the overall interface zone of the concrete.

3.2. Characterisation of concrete during accelerated durability tests

3.2.1. Freeze/thaw cycle tests

The concrete cores drilled from the blocks were subjected to 58 and 85 cycles of freeze/thaw (-18°C to 4°C) according to the ASTM C 666 standard. Non-destructive linear and nonlinear acoustic measurements were performed to assess the variations of concrete properties. The results obtained from UPV and E_{dyn} (in percentage) are shown in Fig. 6 below.

After 58 freeze/thaw cycles, C1-type concrete showed a reduction of 16% of E_{dyn} and a reduction of 2.3% of UPV. After 85 cycles, there was a 20% drop in E_{dyn} and an 8% drop in UPV. C2-type concrete under went more severe degradation, causing a reduction of 29% of E_{dyn} and 11% of UPV after 58 cycles, and a reduction of 27% of UPV after 85 cycles (we were unable to determine E_{dyn} after 85 cycles because the samples were severely damaged and crumbling). These results indicate that the concrete incorporating higher levels of sediment showed lower resistance to freeze/thaw cycles. The measurement of offset frequency in the nonlinear resonance tests also showed degradation of the mechanical properties of the concrete with the addition of fine sediment (Fig. 7). It is of note that this parameter is highly sensitive to variations of concrete stiffness, primarily due to cracking. For C1 samples, an offset frequency increase of 397% was measured after 58 cycles, and 1265% after 85 cycles. C2 samples showed a major increase of offset frequency: 5500% after 58 cycles. Measurements after 85 cycles were not possible because the C2 samples were crumbling.

The impact of freeze/thaw cycles on a cementitious matrix depends on the geomorphological origin of the aggregates, shape and arrangement of pores, cooling rate and repetition of freeze/thaw cycles and saturation of pores [42]. The results of the initial porosity of C1 and C2 (Fig. 6) could partially explain the results in terms of freeze/thaw resistance.

These aspects of both concretes after freeze/thaw cycles are depicted in Figs. 8 and 9. After 58 cycles, the C1 sample shows slight deterioration with the appearance of spalling on the surface. After 85 cycles, substantial cracks show on the surface

Table 3
Mechanical characterisation of tested core samples under non-destructive tests.

	C1	C2	% decrease
UPV(m/s)	3900	3600	7.7 %
E_{dyn} (GPa)	33	28	15.2%
αf	10338	8272	20%

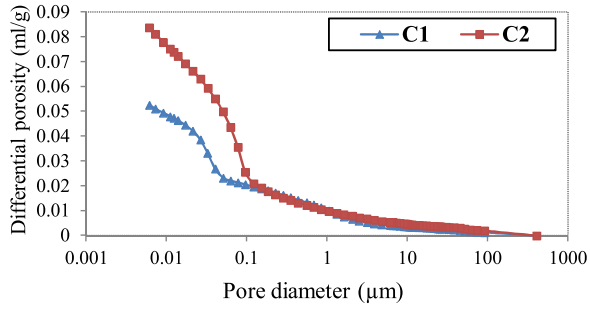


Fig. 3. Average accumulated porosity curve for C1 and C2.

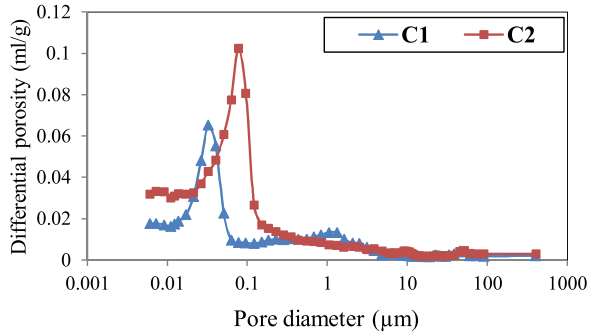


Fig. 4. Average differential porosity curve for C1 and C2.

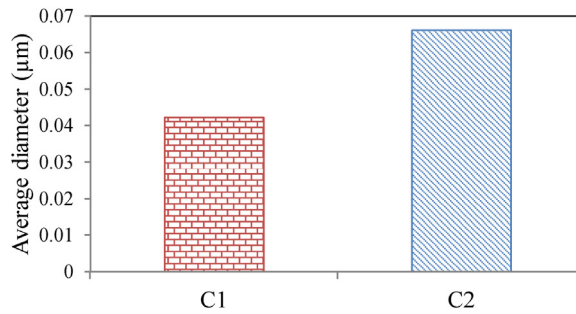


Fig. 5. Average pore diameter in C1 and C2.

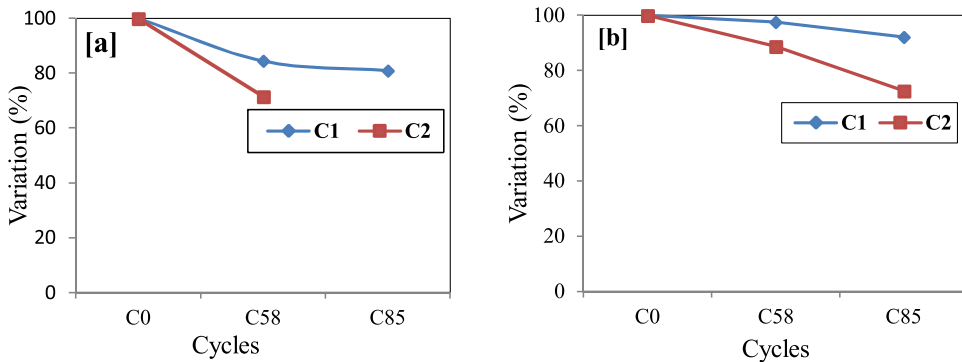


Fig. 6. Variation of linear acoustic parameters for (a) dynamic modulus of elasticity and (b) UPV after 58 and 85 freeze-thaw cycles.

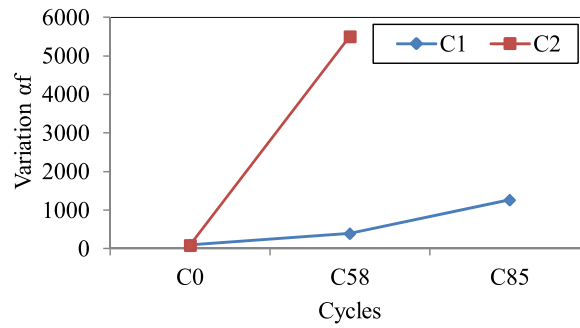


Fig. 7. Variation of the nonlinear acoustics parameter " αf " after 58 and 85 of freeze/thaw cycles (at 85 cycles, C2 concrete became too deteriorated to perform measurements).

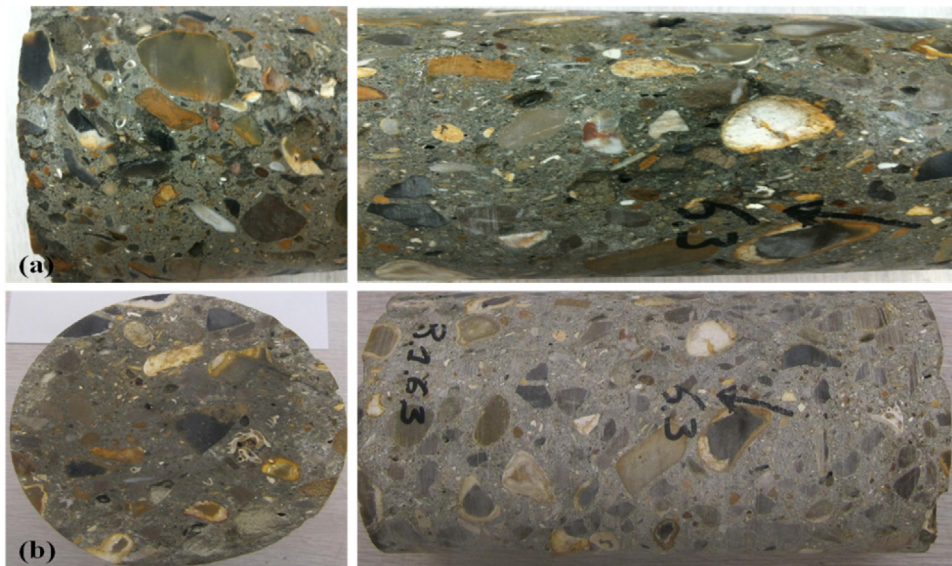


Fig. 8. Sample of C1 after (a) 58 cycles and (b) 85 cycles of freezing/thawing.

and around the edges. The deterioration of the C2 sample is much more pronounced after 58 cycles, with visible surface spalling and deterioration of the edges. Degradation is worse after 85 cycles, with disappearance of chunks of concrete as well as holes left by agglomerates of sediments.

3.2.2. External sulphate attack

3.2.2.1. Total immersion protocol. Samples C1 and C2 were continuously immersed in a 5% $\text{Na}_2\text{SO}_4 \cdot 10\text{H}_2\text{O}$ solution at 23 °C. After five months of total immersion, no particular visual alterations were detected in either type of concrete. Mass variation of samples was measured regularly during the test. Fig.10 shows an increase in mass in both concretes after five months of immersion. For the C1 samples, an increase in mass of 1.5% was recorded, whereas 2% was recorded for the C2 samples. The gain in mass may have been due to water filling the cracks or the porosity of the samples, but it also may have been due to the formation of ettringite [43]. It is also of note that no leaching effects due to the action of the solution on the samples were observed in these tests, likely counter balanced by the increase in mass (as explained above) or the age of the concrete samples. As previously mentioned, the samples investigated in this paper were cored in accropode blocks cast three years previous and were kept in service condition on site. In terms of variation of mechanical properties, a decrease of dynamic modulus of elasticity (E_{dyn}) for C1 and C2 samples was recorded (Fig. 11). This decrease was about 30% for the C1 samples and 28% for the C2 samples. The decrease in E_{dyn} and swelling in both types of concrete are consistent with the start of damage caused by cracking [44,45].

To evaluate the extent of deterioration in the samples and determine the effect of porosity on both types of sediment-based concrete exposed to external sulphate attack, porosity measurement was carried out on deteriorated specimens. Mercury porosimetry results for samples C1 and C2 are shown in differential curves. Fig. 12 below shows a comparison



Fig. 9. Sample of C2 type concrete after (a) 58 cycles and (b) 85 cycles of freeze/thaw.

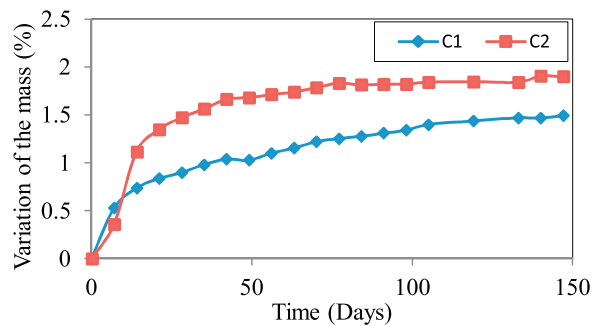


Fig. 10. Variation of average density.

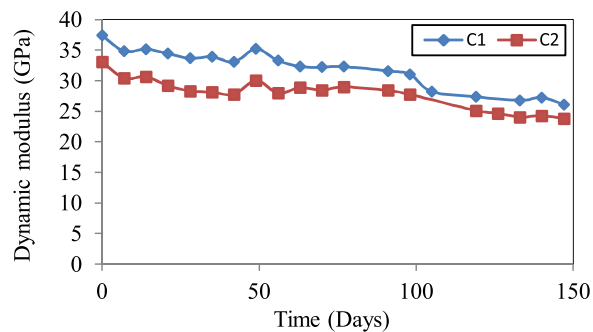


Fig. 11. Variation in the average dynamic modulus of elasticity.

between the differential porosity curves of the C1 concrete prior to deterioration ($T=0$), after one month of total immersion ($T=1$) and after two months of total immersion ($T=2$). Fig. 13 shows the results for C2.

The results show a slight difference between C1 and C2 after two months of total immersion. In both concretes, the main pore size distribution is in the 0.05 to $0.1 \mu\text{m}$ range for the concrete with 12.5% sediment and between 0.08 and $0.2 \mu\text{m}$ for C2. This difference is associated with the percentage of sediment in the C2 concrete.

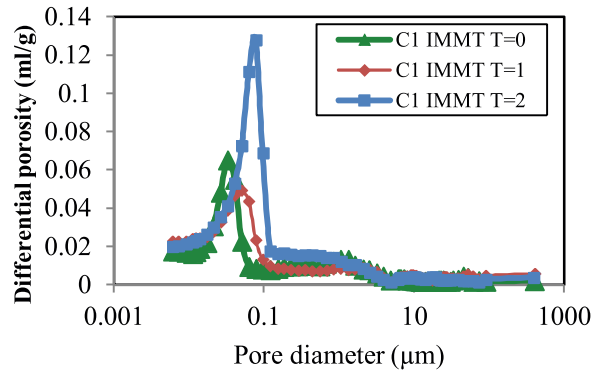


Fig. 12. Variation in differential porosity in C1 in total immersion.

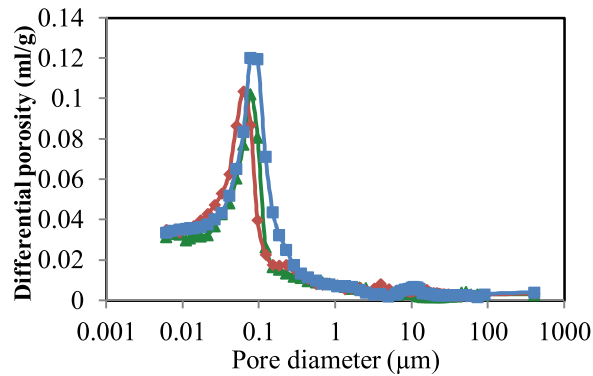


Fig. 13. Variation in differential porosity in C2 in total immersion.

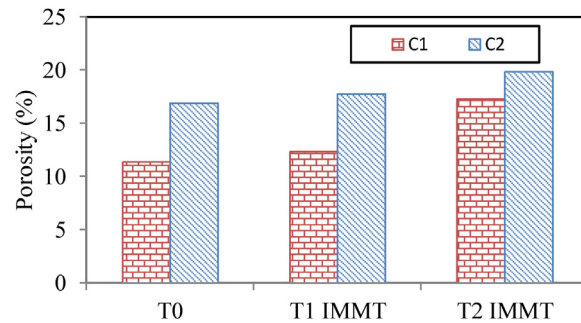


Fig. 14. Comparison of C1 and C2 porosities in total immersion.

Fig.14 shows the differential porosity obtained over the two months of exposure. There is a 5.9% increase in porosity for C1 and a 3.0% increase in C2 during total immersion in a sulphate solution.

3.2.2.2. *Immersion/drying at 105 °C.* During application of the immersion/drying protocol at 105 °C, macroscopic symptoms appeared very early on in the samples. In the C1 samples, deterioration was observed by the fourth week, with deboning at the edges causing cracking. The C2 samples exhibited damage by the third week, with several cracks on the surface of the cores.

After four months of immersion/drying cycles, the C1 samples were completely deteriorated, with damage observed at the surface and at the edge and considerable loss of material. Degradation depth was about 10 mm. Aggregates and sediment pellets could be easily removed; concrete C1 lost part of its cohesion, releasing fragments of paste and aggregates from its granular skeleton.



Fig. 15. Total degradation of C2 after three months of immersion/drying cycles at 105 °C.

Severe deterioration of C2 samples was observed in the third month (one month before the deterioration in C1), consisting of a remarkable loss of material from the surface and edges. Flaws visible to the naked eye consisted of a network of multi-directional cracks at the surface of the cores and other cracks found at the interfaces between the cement paste. The appearance of various surface cracks considerably weakened the material and caused spalling on the surfaces. Swelling and debonding of aggregates was also found and spalling gradually occurred throughout the mass until the C2 concrete had become friable (Fig.15).

Mass variations in the samples are shown in Fig. 16 below. All samples suffered a loss of mass: 4% for C1 and 4.2% for C2 up to the third week. After the third week, both C1 and C2 showed an increase in mass. C2 showed a 1% gain in mass after 11 weeks. After 15 weeks, C1 showed a 2.4% gain. These results suggest that the significant loss of mass measured during the first three weeks is associated with the crack formation in all of the C1 and C2 cores. Delayed ettringite formation (DEF) may have caused expansion and swelling in both types of concrete. Swelling was likely due to the crystallization pressures from the ettringite. The formation of expansive products, such as secondary and delayed ettringite, often leads to disorders and cracks in a cement matrix [46].

A dramatic decrease in E_{dyn} was observed in both types of concrete. After 15 weeks, a loss of 27 GPa total was recorded for C1. C2 suffered a 21 GPa loss after 11 weeks, and then became completely degraded (Fig.17).

The degradation of C1 and C2 into a sulphate environment was likely associated with dissolution of calcium compounds in the hydrated binder and sediment pellets. This phenomenon was observed on the cores tested, with the disappearance of sediment pellets leaving empty spaces on the surface and thereby increasing the number of cracks. The phenomenon was more visible on C2 cores than on C1 cores. Alternate cycles of wetting and drying at 105 °C accelerated the damage caused by salt crystallization in the pores of both concretes. The consequences of sulphate attack were not only swelling, mass variation and cracking, but also a loss of rigidity in both concretes due to a loss of cohesion in the hydrated cement paste and debonding of the cement paste, aggregates and sediment pellets. The accelerated degradation of C2 is likely associated with increased permeability and porosity due to deep cracking. Another phenomenon that may have caused considerable

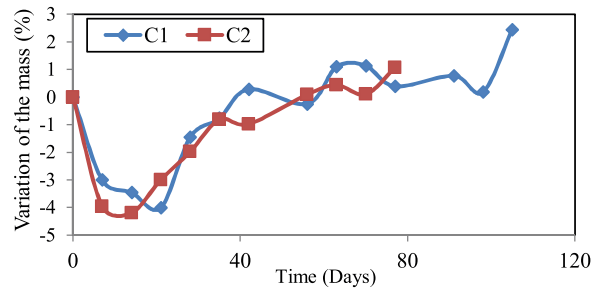


Fig. 16. Average mass variation (Drying at 105 °C).

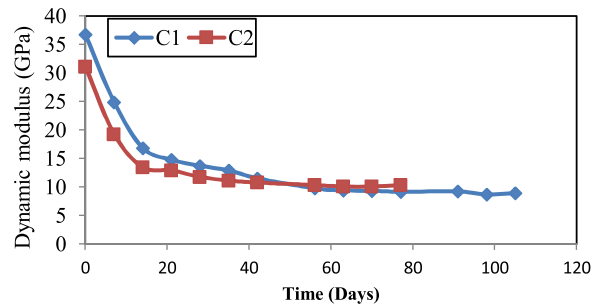


Fig. 17. Average variation in the dynamic modulus of elasticity (Drying at 105 °C).

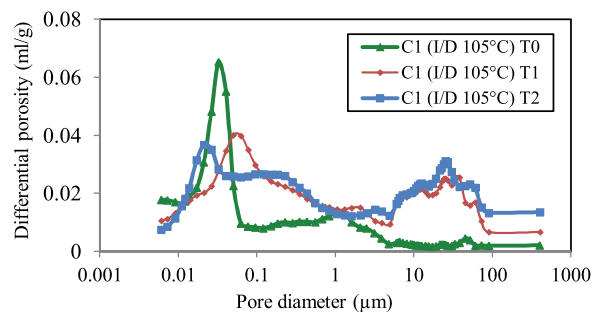


Fig. 18. Differential porosity variation in C1 after immersion-drying cycles at 105 °C.

degradation in both concretes is delayed ettringite formation due to the reaction of sulphate ions with the aluminates in the cement. In fact, ettringite formation generates swelling stresses and deep cracks as observed in concretes C1 and C2.

Fig. 18 below compares the differential porosity curves for the C1 samples initially ($T=0$), after one month of immersion-drying cycles at 105 °C ($T=1$) and after two months ($T=2$). Fig. 19 shows the results for concrete C2.

Analysis of the curves suggests that damage was caused by the progression of cracks and increase in pore volumes. Examination of C1 shows evolution between its initial, undamaged state and its state after two months of cycle exposure, that is, an increase in pore volume from 0.06 to 0.5 μm in the first month and from 0.06 and 1 μm to between 10 and 100 μm by the end of the second month. This major change in the microstructure of C1 indicates that the concrete experienced severe external sulphate attack. C2 also showed an increase in pore volume of between 0.06 and 0.5 μm and between 10 and 90 μm during the first month, indicating a significant microstructural change in the second month with the formation of large pore volume, as compared to its initial, undamaged state. Microstructural change in the concrete in the form of increased porosity is behind the reduction in mechanical properties in both types of concretes and the cracking observed at the start of the immersion-drying cycles at 105 °C. Fig. 20 compares the porosity of both concretes at $T=0$, at one month and two months of immersion-drying cycles at 105 °C. The evolution in the porosity of both concretes shows that they were severely affected by external sulphate attack. The results of this study confirm that the formation of ettringite causes stress cracks and intense swelling. Expansion due to ettringite generated a porous network and tensile pressure causing expansion, cracking or splitting [47].

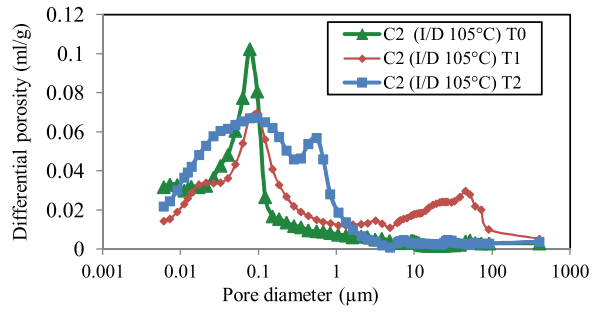


Fig. 19. Differential porosity variation in C2 after immersion-drying cycles at 105 °C.

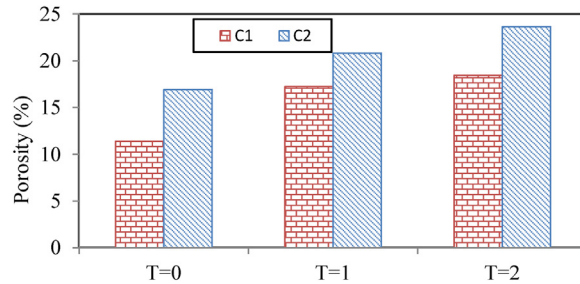


Fig. 20. Comparison of C1 and C2 porosities after immersion-drying cycles at 105 °C.

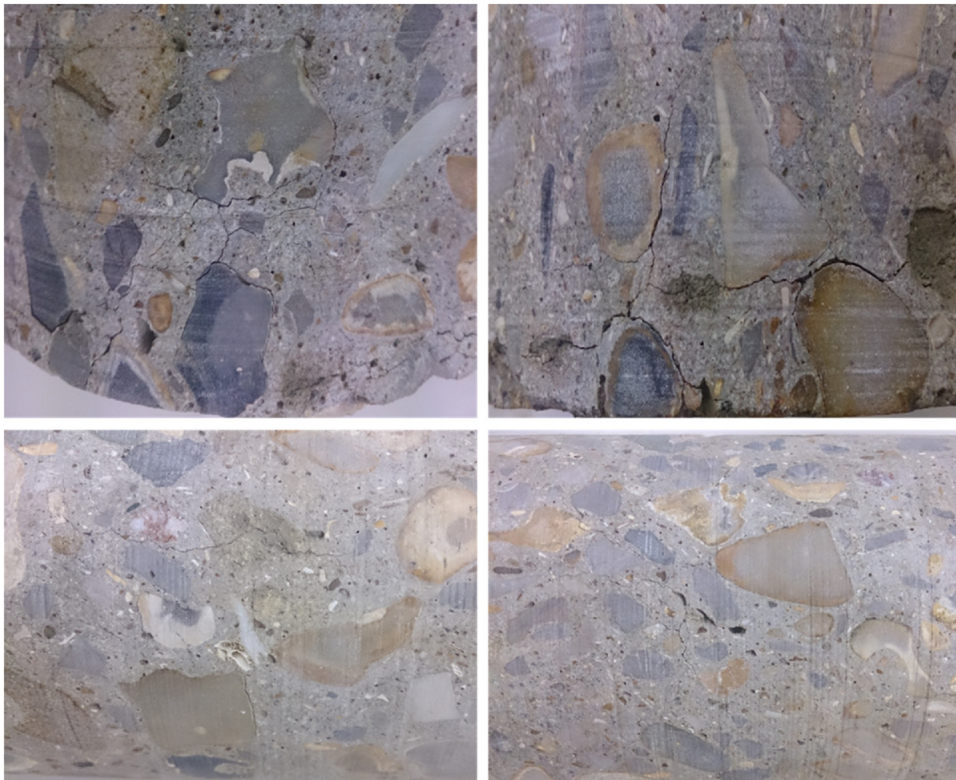


Fig. 21. Degradation and cracking of C1 after 6 months of immersion/drying at 60 °C.

The results show that porosity plays an important role in the degradation caused by external sulphate attack. Porosity increased very significantly in both concretes during the first month of immersion-drying cycles at 105 °C. It caused many empty spaces, visible cracking and pores, which helps sulphates to accumulate and crystallize, generating the swelling and cracking of the concrete.

3.2.2.3. Immersion/drying at 60 °C. In the third protocol study, immersion/drying at 60 °C, deep cracks were observed at the surface and degradation on the edges of C1 after the sixth month and of C2 in the fifth month (Figs. 21 and 22). The cracks were mainly found in the paste, aggregate and sediment pellet interfaces. As observed in the previous protocol, C2 samples showed greater sensitivity to external sulphate attack than C1 samples.

Note that mass variations are similar for both types of concrete. By the 50th day, C1 underwent a maximum loss of 1.7% as compared to a 1.4% loss for C2. In relation to the initial mass, by the 50th day we found a 1.2% gain in C1, and in C2, a 1.5% gain after five months. Concrete C2 showed a larger mass gain than C1 (Fig. 23).

Evaluation of E_{dyn} is shown in Fig. 24. The results showed a drop over time in E_{dyn} for both concretes. C1 showed better resistance than C2. The high level of marine sediment in C2 influenced the properties of the concrete and accelerated its degradation. Comparison of the results of immersion-drying at 60 °C and at 105 °C showed that the 60 °C protocol did not cause formation of DEF.

Fig. 25 compares the three different porosity curves for the initial, undamaged concrete ($T=0$), after one month of immersion-drying at 60 °C ($T=1$) and after two months ($T=2$) for C1. Fig. 26 shows the results for C2.

Analysis of the C1 samples shows a diameter of 0.06 μm in its initial, undamaged state, which increases after one month of attack to 0.1 μm and then around 0.1 μm in the second month, with an increase in pore volume of between 8 and 100 μm . Increased porosity in C1 shows that the concrete has undergone an external sulphate attack, which caused a change in its microstructure. C2 experienced the same effect as C1, an increase in pore volume between 0.01 and 0.11 μm and between 8

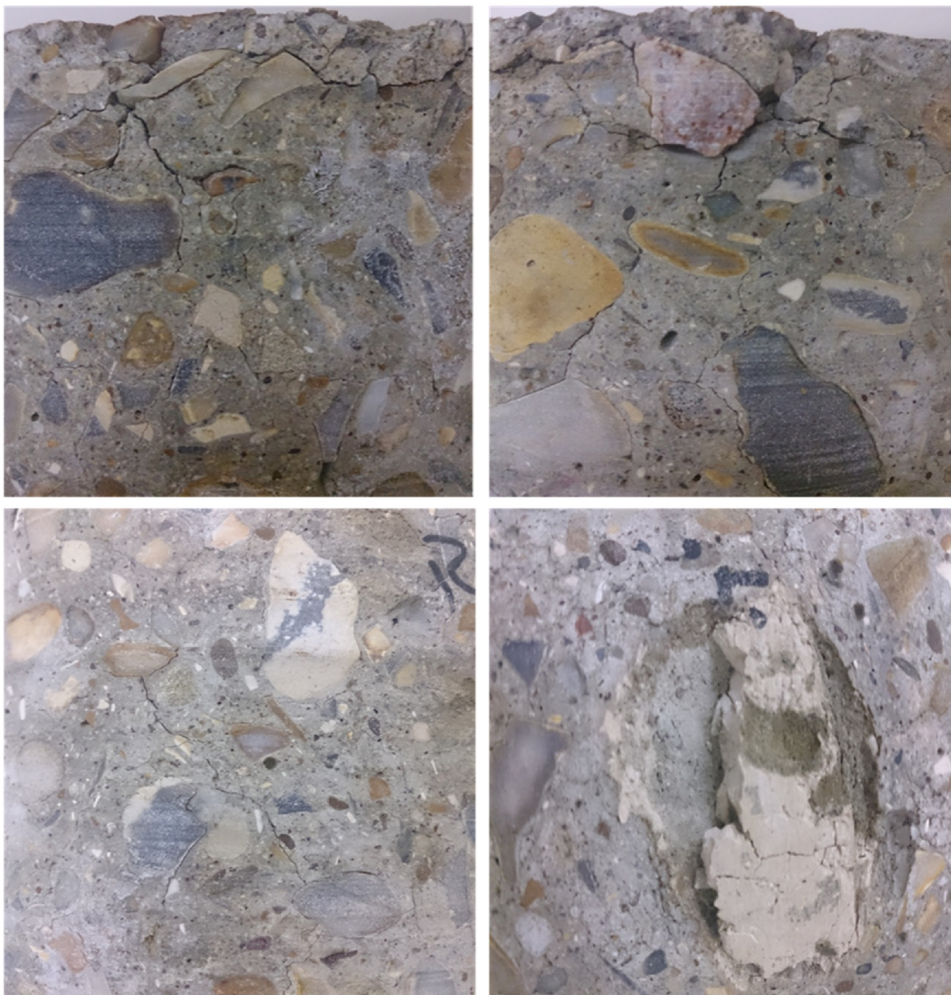


Fig. 22. Degradation and cracking of C2 after 6 months of immersion/drying at 60°.

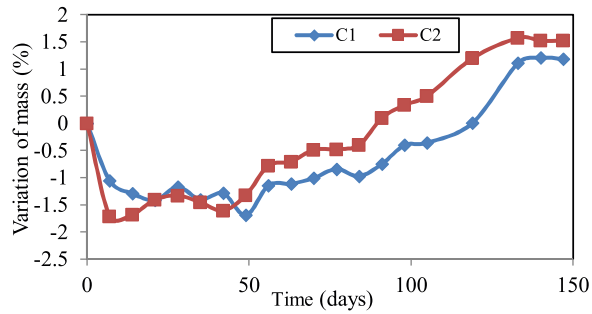


Fig. 23. Average mass variation in C1 and C2 (Drying at 60 °C).

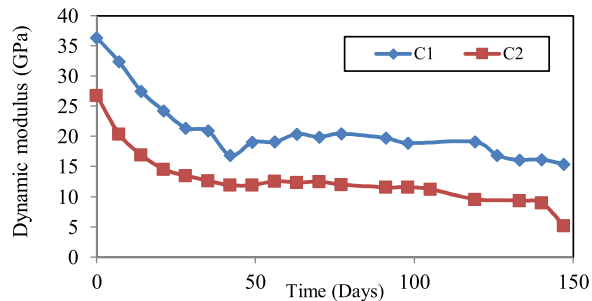


Fig. 24. Variation in the dynamic modulus of elasticity in C1 and C2 (Drying at 60 °C).

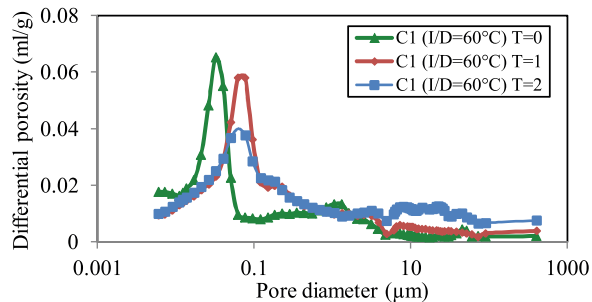


Fig. 25. Variation in differential porosity in C1 after immersion-drying at 60 °C.

and 90 μm during the two months of immersion-drying cycles at 60 °C in relation to the undamaged state. Microstructural changes in both types of concrete due to increased porosity may be the indicator for the reduction of mechanical properties.

Fig. 27 compares the porosity variation in C1 and C2 during two months of immersion-drying cycles at 60 °C. The effect of the alternate cycles led to a 3% increase in porosity in both C1 and C2. The evolution of porosity in the concrete shows that both C1 and C2 were affected by DEF.

3.2.3. Alkali-aggregate reaction tests

Expansions and mass variation measured on concretes C1 and C2 stored at 38 °C are shown in Fig. 28 below.

The various tests carried out on samples of two different formulations of concrete in this study show that increasing expansion and mass variation were observed with increasing proportions of marine sediments in concrete mixtures. Significant expansion was seen in the extremely reactive C2 concrete composed of 20% sediment, while the C1 concrete composed of 12.5% sediment did not show significant expansion or mass variation. Concrete blocks incorporating 20% marine sediment showed high expansion levels (0.07%) and high mass variation (0.8%) over 17 weeks, which likely used a fair amount of reactive silica within the natural aggregate particles.

According to Murlidhar [48], the alkali-silica reaction or alkali carbonates may take place in aggregates such as dredged sediments due to their sand-lime nature.

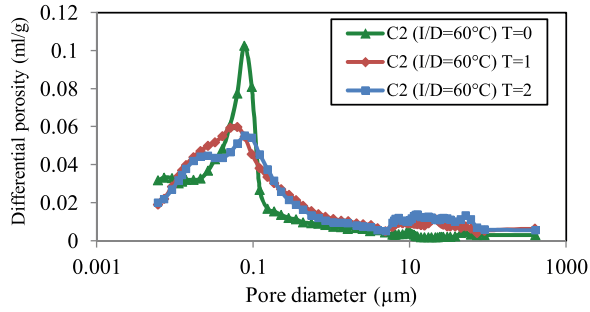


Fig. 26. Variation in differential porosity in C2 after immersion-drying at 60°C.

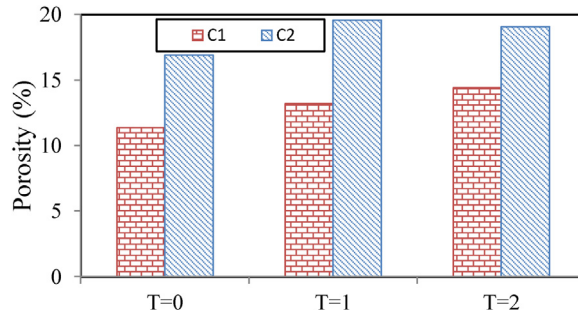


Fig. 27. Comparison of porosities in C1 and C2 following immersion-drying cycles at 60°C.

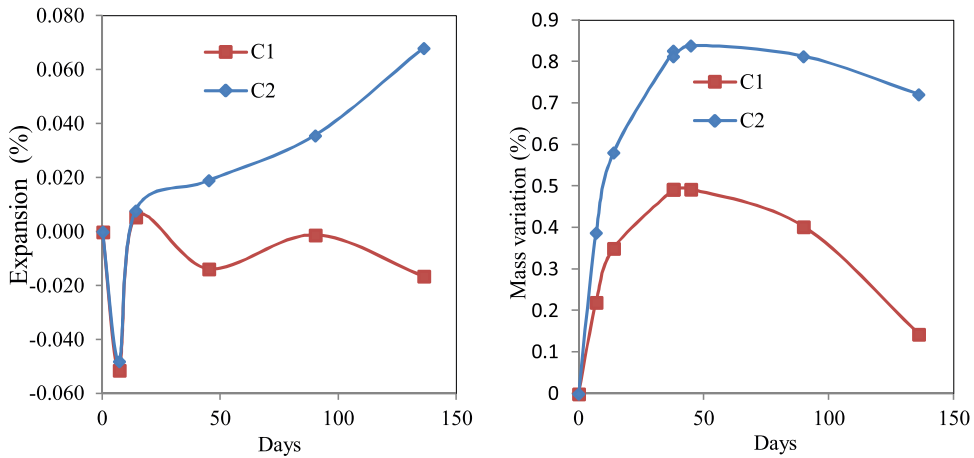


Fig. 28. Expansion and mass variation of samples subject to alkali-aggregate reaction test.

4. Conclusions

This article addresses issues related to marine sediment management and the major economic and environmental issues associated with non-submersible sediments. The study focused on two concrete mixtures incorporating 12.5% (C1) or 20% (C2) marine sediment. Characterisation of both types of concretes showed that, at least from the point of view of mechanical properties, both types can be used in manufacturing accropode blocks. In qualitative comparison, destructive and non-destructive tests showed that the quality of concrete deteriorates with the increase of the amount of fine sediments in the design. The decrease in mechanical properties with the increase of fine dredged sediments is directly associated with the increase of the porosity of the concrete. This phenomenon maybe induced by the effect of dredged sediment on the

compacity of concrete and/or the effect of fine sediments on the rheology of fresh concrete. However, on the basis of the results obtained from both concretes, both could be appropriate for use in manufacturing concrete blocks.

Notably, the results of the durability study show substantial differences in the behaviours of the two kinds of core samples. C1 concrete showed better resistance to freeze/thaw cycles than C2 concrete. The results could also be associated with the porosity exhibited by both types of concrete. In terms of loss of mechanical properties, C1-type concrete exhibited a loss of rigidity in the range of 20%. It is also interesting to note that measurement of the offset frequency α_f seems more sensitive to the harmful effect of freeze/thaw cycles on concrete. This finding needs more exploration.

Exposure to external sulphate attack followed three different protocols: total immersion in a 5% $\text{Na}_2\text{SO}_4 \cdot 10\text{H}_2\text{O}$ solution, immersion/drying cycles at 60 °C and immersion/drying cycles at 105°. The results obtained from the three protocols show that C1 had better resistance than C2 to external sulphate attack. Microstructural analysis of porosity showed increased porosity in C2 as compared to C1. It is also important to note the differences observed in property degradation following the three different protocols. Introducing drying cycles into the protocol likely accelerated the formation of expansive products in the concrete and hence induced severe degradation in the samples. In the case of accropode blocks in contact with seawater, this phenomenon of drying and wetting with seawater will be experienced by the blocks.

Overall, the results obtained in this study suggest that marine sediments can be used in concrete. However, a maximum tolerance of around 12.5% marine sediment substitution would be recommended.

Conflict of interest

The authors declare that there are no conflict of interest.

Acknowledgements

This research was conducted as part of a project to develop alternative solutions for dredged fine sediment management sponsored by the program SEDIMATRERIAUX. This support is gratefully acknowledged, and we would like to thank Harbour of Dunkirk, for his support. The financial support of the Natural Science and Engineering Research Council of Canada (NSERC) is also acknowledged.

References

- [1] V. Dubois, N.E. Abriak, R. Zentar, G. Ballivy, The use of marine sediments as a pavement base material, *Waste Management* 29 (2009) 774–782, doi: <http://dx.doi.org/10.1016/j.wasman.2008.05.004>.
- [2] R. Zentar, N.-E. Abriak, V. Dubois, M. Miraoui, Beneficial use of dredged sediments in public works, *Environ. Technol.* 30 (8) (2009) 841–847, doi: <http://dx.doi.org/10.1080/09593330902990139>.
- [3] R. Zentar, V. Dubois, N.-E. Abriak, Mechanical behaviour and environmental impacts of a test road built with marine dredged sediments, *Resour. Conserv. Recycl.* 52 (2008) 947–954, doi: <http://dx.doi.org/10.1016/j.resconrec.2008.02.002>.
- [4] M. Miraoui, R. Zentar, N.-E. Abriak, Road material basis in dredged sediment and basic oxygen furnace steel slag, *Constr. Build. Mater.* 30 (2012) 309–319, doi: <http://dx.doi.org/10.1016/j.conbuildmat.2011.11.032> ISSN 0950-0618.
- [5] R. Achour, N.-E. Abriak, R. Zentar, P. Rivard, P. Gregoire, Valorisation of unpermitted sea disposal dredged sediments as a road foundation material, *Environ. Technol.* (2014).
- [6] P.X. Pinto, S.R. Al-Abed, E. Barth, C. Loftspring, J. Voit, P. Clark, A.M. Ioannides, Environmental impact of the use of contaminated sediments as partial replacement of the aggregate used in road construction, *J. Hazard. Mater.* 189 (2011) 546–555.
- [7] D.X. Wang, N.E. Abriak, R. Zentar, W.Y. Xu, Solidification/stabilization of dredged marine sediments for road construction, *Environ. Technol.* 33 (2012) 95–101.
- [8] R. Zentar, D. Wang, N.E. Abriak, M. Benzerzour, W. Chen, Utilization of siliceous–aluminous fly ash and cement for solidification of marine sediments, *Constr. Build. Mater.* 35 (2012) 856–863.
- [9] Z. Lafhaj, M. Samara, F. Agostini, L. Boucard, F. Skoczylas, G. Depelseinaire, Polluted river sediments from the North region of France: treatment with the Novosol process and valorisation in clay bricks, *Constr. Build. Mater.* 22 (2008) 755–762.
- [10] M. Samara, Z. Lafhaj, C. Chapiseau, Valorization of stabilized river sediments in fired clay bricks: factory scale experiment, *J. Hazard. Mater.* 163 (2009) 701–710.
- [11] F. Agostini, Inertage et valorisation des sédiments de dragage marins, (2006) .
- [12] E. Rozière, M. Samara, A. Loukili, D. Damidot, Valorisation of sediments in self-consolidating concrete: mix-design and microstructure, *Constr. Build. Mater.* 81 (2015) 1–10.
- [13] N. Junakova, J. Junak, M. Balintova, Reservoir sediment as a secondary raw material in concrete production, *Clean Technol. Environ. Policy* 17 (2015) 1161–1169, doi: <http://dx.doi.org/10.1007/s10098-015-0943-8>.
- [14] J.L. Dalton, K.H. Gardner, T.P. Seager, M.L. Weimer, J.C.M. Spear, B.J. Magee, Properties of Portland cement made from contaminated sediments, *Resour. Conserv. Recycl.* 41 (2004) 227–241, doi: <http://dx.doi.org/10.1016/j.resconrec.2003.10.003>.
- [15] G. Aouad, A. Laboudigue, N. Gineys, N.E. Abriak, Dredged sediments used as novel supply of raw material to produce Portland cement clinker, *Cem. Concr. Compos.* 34 (6) (2012) 788–793, doi: <http://dx.doi.org/10.1016/j.cemconcomp.2012.02.008> ISSN 0958-9465.
- [16] H. Azrar, R. Zentar, N.-E. Abriak, The effect of granulation time of the pan granulation on the characteristics of the aggregates containing dunkirk sediments, *Procedia Eng.* 143 (2016) 10–17, doi: <http://dx.doi.org/10.1016/j.proeng.2016.06.002> ISSN 1877-7058.
- [17] M. Amara, M. Benzerzour, A. Safhi, N.-E. Abriak, Durability of a cementitious matrix based on treated sediments, *Case Stud. Constr. Mater.* 8 (2018) 258–276.
- [18] F.K. Aoual-Benslafa, D. Kerdal, M. Ameer, B. Mekerta, A. Semcha, Durability of mortars made with dredged sediments, *Procedia Eng.* 118 (2015) 240–250.
- [19] Z. Zhao, M. Benzerzour, N.-E. Abriak, D. Damidot, L. Courard, D. Wang, Use of uncontaminated marine sediments in mortar and concrete by partial substitution of cement, *Cem. Concr. Compos.* 93 (2018) 155–162, doi: <http://dx.doi.org/10.1016/j.cemconcomp.2018.07.010> ISSN 0958-9465.
- [20] Essais pour béton dans les structures – Partie 1 : Carottes – Prélèvement, examen et essais en compression, AFNOR, 2019 NF EN 12504-1.
- [21] ASTM C, Standard Test Method for Compressive Strength of Cylindrical Concrete Specimens, Norme ASTM 39-02, (2019) .
- [22] ASTM C, Standard Test Method for for Splitting Tensile Strength of Cylindrical Concrete Specimens, Norme ASTM 496-04, (2019) .

- [23] ASTM C, Standard Test Method for Static Modulus of Elasticity and Poisson's Ratio of Concrete in Compression 469-02, (2019) .
- [24] J. Mazars, Application de la mécanique de l'endommagement au comportement non linéaire et à la rupture du béton de structure, Thèse 6, University of Paris, 1984.
- [25] L.F. Nielsen, Strength development in hardened cement paste: examination of some empirical equations, *Mater. Struct.* 26 (1993) 255–260, doi:<http://dx.doi.org/10.1007/BF02472946>.
- [26] ASTM C, Standard test for pulse velocity through concrete, norme ASTM 597-97, (2019) .
- [27] ASTM C, Standard Test Method for Fundamental Transverse, Longitudinal, and Torsional Frequencies of Concrete Specimens, Norme ASTM 215-02, (2019) .
- [28] P. Rivard, F. Saint-Pierre, Assessing alkali–silica reaction damage with non-destructive methods: from the lab to the field, *Constr. Build. Mater.* 23 (2) (2009) 902–909.
- [29] A.S. Kodjo, Contribution to the Characterization of Damaged Concrete With Nonlinear Acoustics: Application to Alkali–silica Reaction, (Ph.D. Thesis), Université de Sherbrook/Université Cergy-Pontoise, 2009 (127 pages).
- [30] ASTM C666, Standard Test Method for Resistance of Concrete to Rapid Freezing and Thawing, norme ASTM, (2019) .
- [31] J. Skalny, J. Marchand, I. Odler, Sulphate Attack on Concrete, Spon Press, London, 2002.
- [32] P. Kumar Mehta, Sulfate attack on concrete separating myths from reality, *Concr. Int.* 22 (2000).
- [33] A. Neville, The confused world of sulphate attack on concrete, *Cem. Concr. Res.* 34 (8) (2004) 1275–1296.
- [34] P.C. Hewlett (Ed.), *Lea's Chemistry of Cement and Concrete*, Arnold, London, 1998.
- [35] A.M. Neville, *Propriétés des bétons* Editions Eyrolles, 806pp. ISBN : 2-212-01320-5, (2000) .
- [36] B. Fournier, M.-A. Bérubé, Alkali-aggregate reaction in concrete: a review of basic concepts and engineering implications, *Can. J. Civ. Eng.* 27 (2000) 167–191.
- [37] Potential Expansivity of Aggregates; Procedure for Length Change Due to Alkali-Aggregate Reaction in Concrete Prisms, (2019) CAN/CSA-A23.2-14A-14 [See A23.2-14].
- [38] ASTM, C1293 - 18 Standard Test Method for Determination of Length Change of Concrete Due to Alkali-silica Reaction, (2019) .
- [39] Y. Boukari, D. Bulteel, P. Rivard, N.-E. Abriak, Combining nonlinear acoustics and physico-chemical analysis of aggregates to improve alkali–silica reaction monitoring, *Cem. Concr. Res.* 67 (2015) 44–51.
- [40] M. Sargolzhai, S.A. Kodjo, P. Rivard, J. Rhazi, Effectiveness of non-destructive testing for the evaluation of alkali–silica reaction in concrete, *Constr. Build. Mater.* 24 (2010) 1398–1403.
- [41] V. Baroghel-Bouny, A. Ammouche, «Sous Groupe Microstructure», GranDuBé, 2007) Grandeurs associées à la durabilité des bétons. Presses de l'école nationale des Ponts et Chaussées (ENPC), 2006 Juin 2007.
- [42] S. Forster, S. Moore, M. Simon, Behavior of recycled concrete as aggregate in concrete, *Conf. Durab. Concr. Nice Fr.*, (1994) .
- [43] E. Rozière, A. Loukili, R. El Hachem, F. Grondin, Durability of concrete exposed to leaching and external sulphate attacks, *Cem. Concr. Res.* 39 (12) (2009) 1188–1198 Elsevier.
- [44] X. Brunetaud, M.-R. Khelifa, M. Al-Mukhtar, Size effect of concrete samples on the kinetics of external sulphate attack, *Cem. Concr. Compos.* 34 (2012) 370–376, doi:<http://dx.doi.org/10.1016/j.cemconcomp.2011.08.014>.
- [45] X. Brunetaud, Etude de l'influence de différents paramètres et leurs interactions sur la cinétique et l'amplitude de la réaction sulfatique interne du béton, (Ph.D. thesis), Ecole centrale de Paris, 2005 2005, 253p.
- [46] M. Santhanam, M.D. Cohen, J. Olek, Mechanism of sulphate attack: a fresh look, *Cem. Concr. Res.* 33 (2003) 341–346, doi:[http://dx.doi.org/10.1016/S0008-8846\(02\) 00958-4](http://dx.doi.org/10.1016/S0008-8846(02) 00958-4).
- [47] Bryant Mather, Sulfate Attack On Hydraulic-Cement Concrete, *Spec. Publ.* 2004, pp. 223, doi:<http://dx.doi.org/10.14359/13502>.
- [48] B.R. Murlidhar, E.T. Mohamad, D.J. Armaghani, Potential alkali silica reactivity of various rock types in an aggregate granite quarry, *Measurement* 81 (2016) 221–231, doi:<http://dx.doi.org/10.1016/j.measurement.2015.12.022>.